Received: 19 May 2021 | Revised: 19 November 2021 | Accepted: 11 January 2022

DOI: 10.1002/psp4.12762

TUTORIAL

Streamlining physiologically-based pharmacokinetic model design for intravenous delivery of nanoparticle drugs

Anh-Dung Le[1] | **Helen J. Wearing**[2] | **Dingsheng Li**[3]

[1]Nanoscience & Microsystems Engineering, University of New Mexico, Albuquerque, New Mexico, USA

[2]Department of Biology, Department of Mathematics & Statistics, University of New Mexico, Albuquerque, New Mexico, USA

[3]School of Community Health Sciences, University of Nevada, Reno, Nevada, USA

Correspondence
Anh-Dung Le, Nanoscience & Microsystems Engineering, ZMSC01 1141, University of New Mexico, Albuquerque, NM 87131.
Email: ale@unm.edu

Funding information
No funding was received for this work

Abstract

Physiologically-based pharmacokinetic (PBPK) modeling for nanoparticles elucidates the nanoparticle drug's disposition in the body and serves a vital role in drug development and clinical studies. This paper offers a systematic and tutorial-like approach to developing a model structure and writing distribution ordinary differential equations based on asking binary questions involving the physicochemical nature of the drug in question. Further, by synthesizing existing knowledge, we summarize pertinent aspects in PBPK modeling and create a guide for building model structure and distribution equations, optimizing nanoparticle and non-nanoparticle specific parameters, and performing sensitivity analysis and model validation. The purpose of this paper is to facilitate a streamlined model development process for students and practitioners in the field.

BACKGROUND

Nanoparticles have distinct properties that make them unique in their applications in nanomedicine partly due to the high surface area-to-volume ratios which allow for functionalization of drug nanocarriers. For instance, metallic nanoparticles, such as iron oxide or gold nanoparticles, can be used in medical imaging.[1–3] This rise in the use of nanotechnology in medicine has crossed paths with pharmacology resulting in the need for understanding of biodistribution (distribution throughout the body) of drugs and their carriers.

There are a number of different nanocarriers that have been used in the development of nano drug delivery systems. Hossen et al. reviewed several different nanocarrier drug delivery systems for cancer therapy, including colloidal nanoparticles and liposomes.[4] These nanocarriers have different roles in how they carry the associated drugs throughout the body. For example, colloidal nanoparticles, such as gold nanoparticles, are a good candidate for a drug carrier because they have good biocompatibility and can be conjugated to different molecular species.[5] Further, their optical properties as a result of surface plasmon resonance make it possible for them to be used in imaging purposes.[6] Liposomes can be functionalized to recognize cancer cells while carrying cargos of hydrophilic drugs that can be released upon activation.[4] Other drugs are turned into their nanocrystalline form to overcome the low solubility in both water and oil.[7] Such nanocrystal drugs have a dissolution rate constant that must be taken into account during modeling and simulation.

Biodistribution of nanoparticles can be modeled in silico using pharmacokinetics modeling. Physiologically-based pharmacokinetic (PBPK) modeling takes into account more physiological processes compared to traditional one-compartment pharmacokinetics modeling and is important in the field of pharmacology. The US Food and Drug Administration (FDA) regulates PBPK modeling for regimenting drug dosages in order to safely predict efficacious therapeutic indices for drugs.[8] Moreover, PBPK modeling is also important in the field of environmental science and engineering due to the risk of exposure to toxic nanoparticles and the need for rational design of nanoparticles, respectively. PBPK modeling may be further applied in areas relating to diagnostics, for example, predicting the biodistribution of monoclonal antibodies.[9–11]

PBPK modeling is a powerful tool used in the research and development of drugs partly due to the ability to predict and understand drug behavior. PBPK modeling may be used both, a priori, to mechanistically predict drug disposition, as well as, a posteriori, to empirically understand drug behaviors by estimating parameters.[12] Empirical data may also be used to validate model predictions (Figure 1). PBPK modeling has been used to study the biokinetics of nanoparticle drugs in terms of modeling past experimental data as well as predicting appropriate dosages through simulations.[13–17] However, one major limitation that has been ascribed to PBPK modeling of nanoparticles is the application of the resulting model for only one type of nanoparticle at a time.[18] Every new nanoparticle formulation would require reparameterization due to changes in the physicochemical properties of the particles being used in the model as well as how certain factors such as cell permeability and macrophage uptake rate may be affected. This limitation results in a shortage of models that can keep up with the demands of different types of nanoparticle drugs being developed in the pharmaceutical industry. This paper focuses on providing a unifying framework—to understand how to develop a nanoparticle PBPK model via a systematic approach where major parameters, model compartments, and physiological factors are considered.

COMPARTMENTAL MODEL STRUCTURE

PBPK models can consist of many compartments, for example, including the venous blood, arterial blood, lungs, heart, muscle, brain, kidneys, liver, gut, spleen, adipose tissue, skin, and bones.[19] Some of these compartments may be grouped together depending on their influence on biodistribution.[20] Venous and arterial blood are sometimes considered as one compartment called the plasma or blood circulation.[21] However, other slightly different combinations of compartments, including the lymph nodes and thymus, may also be included, for example.[22,23] Most other PBPK models incorporate a miscellaneous or remainder compartment that may include tissues either insignificant or not sampled to further account for the total amount of mass of the administered dose.[24–27]

PBPK model design often consists of both arterial blood as well as venous blood compartments in order to account for the lag in drug distribution when an i.v. dose is administered.[28] On the other hand, in a single blood circulation compartment, any i.v. dose administered will take on the presumption that the drug will travel directly to all the organs, in other words, having 100% biodistribution much quicker.[29,30] More accurately, in a dual blood circulation compartment, an i.v. injection will typically take place on the accessory cephalic vein, which is located on the back of the arm, delivering the drug at the site of the vein carrying deoxygenated blood.[28] In experiments involving mice, for example, the tail vein is the place of injection into the venous blood.

Figure 2 shows the structures of a typical multicompartment PBPK model currently used across the literature for modeling disposition of nanoparticle drugs. The multicompartment model structure containing separate venous and arterial blood compartments can be slightly modified to describe whether the model is flow-limited or membrane-limited, or whether or not it contains phagocytizing subcompartments, for instance.

In all parts in Figure 2, the multicompartment PBPK model structure utilizes both the venous and the arterial blood compartments instead of only one plasma compartment. However, a model structure that utilizes one plasma compartment for colloidal nanoparticles has also been demonstrated to be effective.[21] Such a model structure would experience latency in the calculated distribution time accounting for blood flowing to the lungs and arterial blood before going to peripheral organs.[28] In dissolvable nanoparticle, membrane-limited structures, a structure similar to that of Figure 2d could be used with the presence of capillary compartments similar to that of Figures 2b and c.

The organ compartments involved in the hepatic portal circulation in Figure 2 are summarized in one compartment for the purpose of illustrating a simplified model structure. However, these different organs have their own designated compartment because they have different parameters such as blood flow, organ volume, permeability coefficients, and partition coefficients. On the other hand, compartments not involved in the pharmacokinetic study will be grouped together in the model

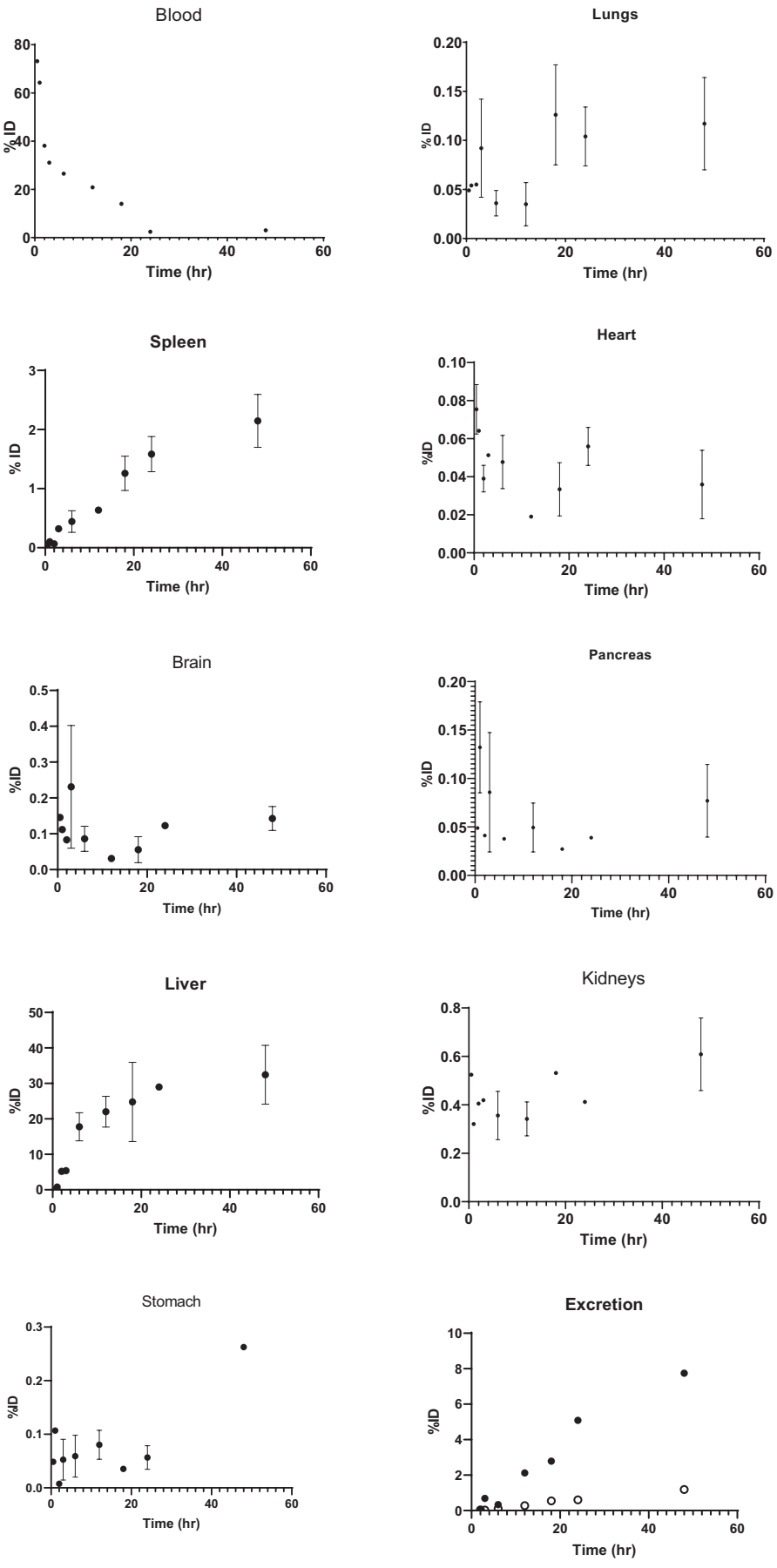

FIGURE 1 The 10 nm PEG 2000 colloidal gold nanoparticle biodistribution in mice after an i.v. injection. Data adapted from Takeuchi et al. The plots shown here are in %ID (percent of initial doses) versus time drug disposition plots

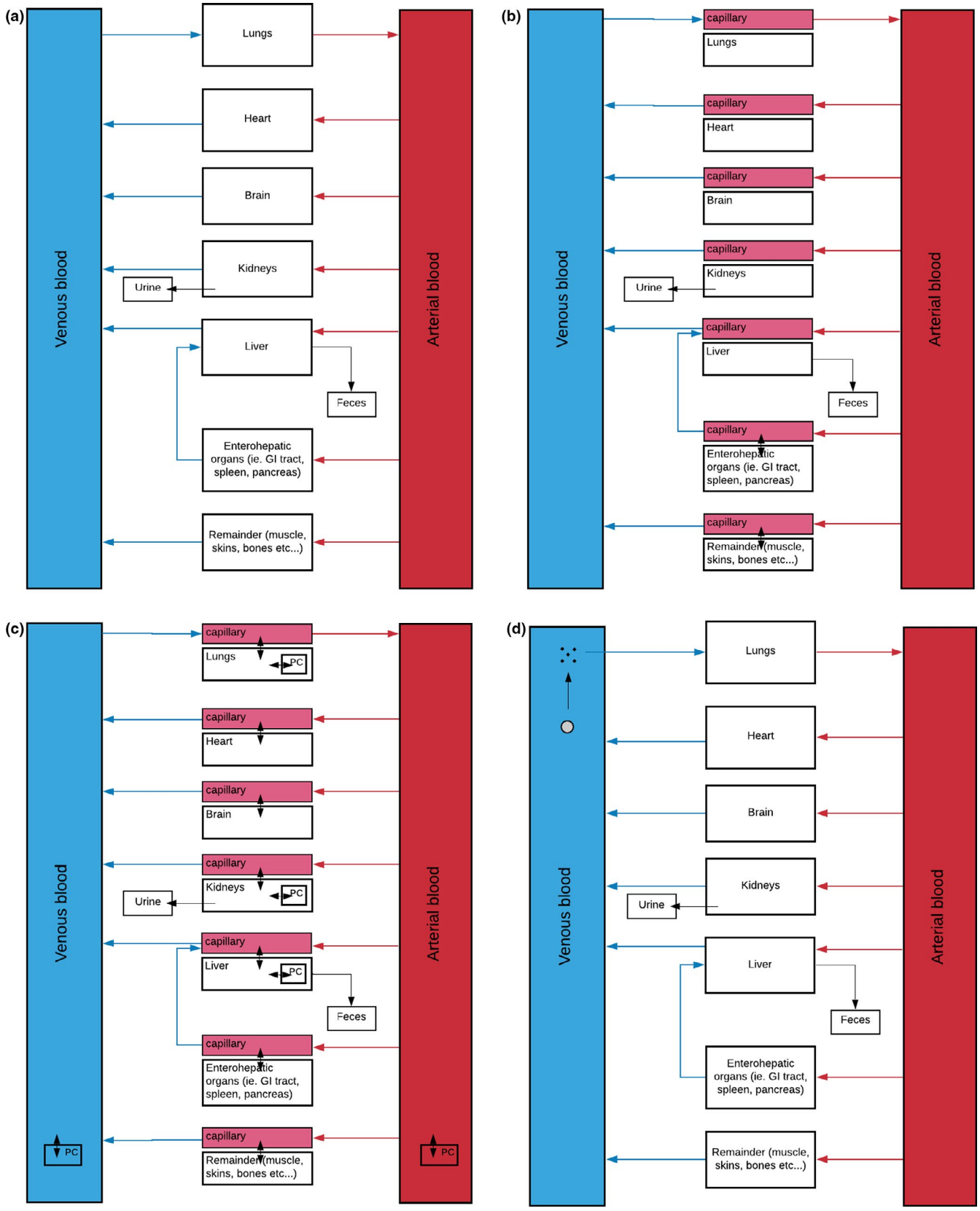

FIGURE 2 Multicompartment PBPK model structures for different hypothetical scenarios. (a) Non-nanoparticle, flow-limited structure (with specific examples found in refs. 25,90); (b) nondissolvable, colloidal-nanoparticle, and membrane-limited structure; (c) nondissolvable, colloidal-nanoparticle, and membrane-limited structure, with phagocytizing cell subcompartments (with specific examples found in refs. 20,31,48); and (d) dissolvable nanoparticle, flow-limited structure (with specific example found in ref. 7). GI, gastrointestinal; PBPK, physiologically-based pharmacokinetic

structure as the remainder compartment. The total organ volume of the remainder compartment will be the difference between the organism's body weight and the weight of the organs already accounted for, including the venous and arterial blood. The blood flow to the remainder compartment should be similar because they are lowly perfused organs, hence a reason for their lack of attention in pharmacokinetic studies. As far as colloidal nanoparticles are concerned, their distribution between organs and the blood circulation is not a reflection of the thermodynamic equilibrium between two immiscible liquids.[31] Therefore, the "partition" coefficient may be the same for similar nanoparticles between the blood and similar tissues.

Mathematical framework

Building upon traditional pharmacokinetic frameworks, PBPK models for nanoparticles would also incorporate specific physiological processes such as macrophage uptake.[7,21,32,33] Distribution equations are used to account for the drug's location within the body after a given amount of time. Depending on whether nanoparticles undergo certain transitional states, the differential equations governing a PBPK model can be affected. For instance, for nanoparticles undergoing dissolution, the distribution equation will need to include a term to account for this drug release process.

The construction of the mathematical distribution equations depends on our knowledge of the physicochemical nature of the drug. In order to build a model that best reflects the underlying biodistribution processes, the modeler should ask questions pertaining to their understanding of the drug formulation, such as:

- Whether it is a hydrophilic or hydrophobic substance;
- Whether it is a small or large molecule;
- Whether the nanoparticles in the formulation will undergo dissolution or not; and
- Whether there is macrophage uptake of the nanoparticles or not.

Imposing these questions as a systematic approach to developing a PBPK model can streamline the model structure development process.

The flow diagram in Figure 3 can be used to construct a PBPK model structure that is consistent with published models reflecting the physicochemical characteristics of a drug. For example, in a model for SNX-2112, a poorly soluble molecular anticancer drug that was formulated into dissolvable nanocrystals for evaluating its disposition in rats, used a release constant (k_{rel}) in the distribution equations, and adopted a flow-limited structure with no phagocytizing cell compartment.[7] In the case of colloidal nanoparticles, nondissolvable nanoparticles are described using membrane-limited model structures with phagocytizing cell subcompartments.[31,34] Equation 1 begins with

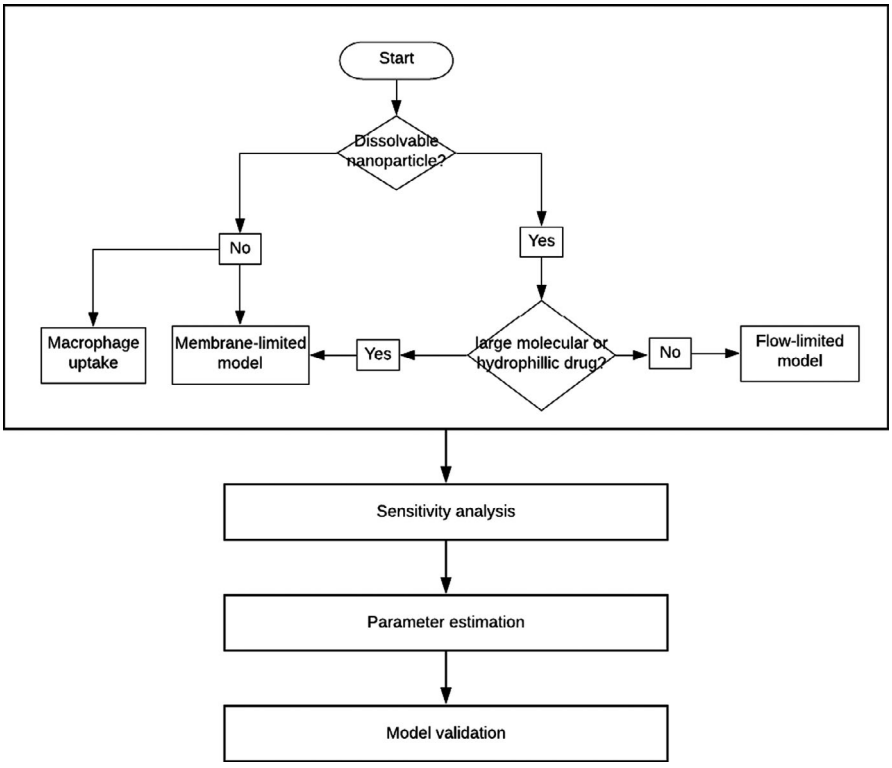

FIGURE 3 Shows a flow diagram of the basic decision-making process in constructing a PBPK mathematical framework. The final mathematical formulation of the differential equation describing the amount of drug in a particular organ compartment on the physicochemical properties of the drug formulation. This process is followed by subsequent steps in the model building process. PBPK, physiologically-based pharmacokinetic

the basic components of the differential equation utilizing the law of mass action:

$$\frac{dM_2}{dt} = Q \times \left(C_1 - \frac{C_2}{k_p} \right) \quad (1)$$

where $\frac{dM}{dt}$ is the rate of change of the amount of drug in compartment 2 at time t; Q, with units of volume per time, is the blood flow from compartment 1 into compartment 2; C_1 and C_2, with units of amount per volume, are the drug concentrations in compartments 1 and 2, respectively; and k_p, with no units, is the partition coefficient. The partition coefficient is the ratio of a substance in two immiscible or slightly miscible solvents in thermodynamic equilibrium. Note that the distribution equation for the plasma compartment applies the partition coefficient toward the concentration of the drugs coming from the lungs and not away from the plasma. This is because partition coefficients are applied to concentration of drugs leaving an organ compartment and into a plasma compartment. In other words, there is no partitioning taking place when drugs enter an organ compartment from the plasma. When applying this coefficient to model construction for colloidal nanoparticles, it is not thermodynamic equilibrium between the tissue compartment and the circulation that the coefficient reflects. Therefore, a better name for partition coefficient in such an instance would be distribution coefficient.[31]

The drug will ultimately be eliminated from the body through either renal excretion where drugs will be excreted from the kidneys into the urine, or biliary excretion where drugs are excreted into the feces by the bile.[35] The clearance rate can vary depending on the drug. The mass equation ultimately includes the summation of both of these processes. Thus, for compartments involving renal or biliary excretion:

$$\frac{dM}{dt} = Q \times \left(C_1 - \frac{C_2}{k_p} \right) - \frac{dM_{ex}}{dt} \quad (2)$$

$$\frac{dM_{ex}}{dt} = \left(M_l \times CL_b + M_k \times CL_r \right) \quad (3)$$

where $\frac{dM_{ex}}{dt}$ in units of amount per time, is the rate of excretion of drugs; M_l is the amount of nanoparticles in the liver tissue; M_k is the amount of nanoparticles in the kidney's capillary blood; CL_b, in units of time^{-1}, is the clearance to feces from the liver tissue; and CL_r, in units of time^{-1} is the clearance to urine from the kidney's capillary blood.

Nanoparticle transitions

In oral administration, whether the drug is subject to quick or slow release, it is only the bioavailability—the proportion of drug that enters the circulation—that has its active effect, which varies from formulation to formulation. It is assumed that once the drug reaches the circulation, its biodistribution does not depend on dissolution kinetics inside the circulation because all of the dissolution has already taken place. Nanoparticle formulations, where cargos of drugs are loaded or where the drug molecules form nanocrystals through self-assembly, for example, require the use of decomposition or dissolution kinetics in formulating a PBPK model, because additional time is needed for the nanoparticle state to decompose or dissolve into the free drug state. Nanoparticle drug delivery systems containing drugs which could later be released in the systemic circulation and in organ compartments, would include a term to describe the transition between the nanoparticle and the dissolved states. This transition may be integrated into PBPK modeling. In this case, release constants are needed in the distribution equations. These constants may be measured or obtained from the literature via prior in vitro studies.

One physiological phenomenon that can affect nanoparticle states is the formation of what was initially coined as protein coronas, which has been studied since at least 2007.[36] It is a phenomenon in which a protein adsorption layer is formed around a foreign colloidal nanoparticle.[36–39] The adsorbed proteins may include fibrinogen, vitronectin, human serum albumin, and cytochrome C.[40] A mechanistic study has shown surface properties of nanoparticles play an important role in determining interactions with the host's immune responses even more so than nanoparticle sizes when these particles are initially introduced into the circulation.[41] The formation of protein coronas involves both hetero- and homo-aggregation, where nanoparticles aggregate with proteins or with themselves, respectively, based on ionic concentration of the environment.[39] The effect of protein coronas can act as a confounding variable affecting cell-specific targeting and uptake of nanoparticles, for example.[42] The formation of this corona layer around nanoparticles does beg the question of whether or not this plays into the kinetics of dissolution, and thus, the PBPK model itself. In fact, some efforts do exist in order to explain the kinetics of the protein corona.[40,43] In light of this knowledge, the pharmacokineticist must decide whether or not to take into account the effects of this protein corona. A global sensitivity analysis may help determine the influence of a parameter, and, in this case, the rate of dissolution of nanoparticulate drugs having a protein corona layer. Understanding that the state of nanoparticulate drugs need to be taken into account will allow the pharmacokineticist to incorporate dissolution equations into the PBPK models. Additionally, nanoparticulate drugs may not always decompose through dissolution, as in the case of nanocrystals of SNX-2112.[7] Rather, they may be released

through other means. For example, drugs may be packaged in mesoporous nanoparticles that can released via various triggering mechanisms.[44] Moreover, nanoparticles may be delivered to the circulation in lipid-based vesicles, via functionalized-gold nanoparticles as carriers, or even in micelles.[45–47] Thus, understanding of the drug release mechanisms of the different formulations is needed in order to take into account the drug release term in the PBPK model. Understanding the chemicophysical properties of the drug (i.e., dissolvable vs. colloidal and membrane-limited vs. diffusion-limited) is crucial in designing the model structure because these properties dictate the inclusion of additional reactions and compartments.

When nanoparticle formulations are used, the release of drugs through dissolution can occur and a release constant is needed in the calculation. However, colloidal nanoparticles used as drug carriers or as contrast agents in magnetic imaging modalities do not undergo dissolution and therefore there will not be any inclusion of dissolution reaction in the model. This can further affect whether the particles will take on a diffusion-limited or membrane-limited structure of the model, for instance.

Dissolvable nanoparticles

Dissolvable nanoparticles undergo dissolution in the aqueous milieu. Therefore, subsequent to an i.v. administration, a first-order release term with constant k_{rel} must be used to account for this dissolution process in the plasma. An example of the utilization of k_{rel} is demonstrated in Wu et al. where biodistribution of nanocrystals of an anticancer agent SNX-2112 was modeled.[7] Where nanoparticle dissolution takes place, a term must be used to account for the change in the amount of dissolved drug with respect to time. Therefore, the distribution equation describing the nanoparticle amount while considering dissolution in compartments will include $-\left(k_{rel} \times V_t \times C\right)$ and the distribution equation describing the corresponding dissolved drug will include $+\left(k_{rel} \times V_t \times C\right)$ such that:

$$\frac{dM_2}{dt} = Q \times \left(C_1 - \frac{C_2}{k_p}\right) \pm \left(k_{rel} \times V_t \times C\right) \quad (4)$$

where V_t is the volume of the compartment where dissolution is taking place and C is the concentration of the nanoparticle drug before dissolution in that compartment (either compartment 1 or 2). Of course, if all nanoparticles dissolve completely in the venous blood compartment (i.e., after i.v. administration), then nanoparticle dissolution will no longer apply to subsequent compartments. However, all of that will depend on the k_{rel} constant.

Colloidal nanoparticles

Colloidal nanoparticles do not dissolve in aqueous milieu and there is no evidence of dissolution in the circulation.[31] Therefore, the release constant is not included. Thus, crossing the membrane into the intracellular fluid would be a rate-limiting step and the distribution equation will be multiplied by a term describing permeability under the membrane-limited framework, as presented previously by Li et al.[48]:

$$\frac{dM}{dt} = Q \times \left(C_1 - \frac{C_2}{k_p}\right) \times \frac{X}{1+X} - \frac{dM_{ex}}{dt} \quad (5)$$

Where X is the unitless permeability coefficient. Notice that the distribution equation is directly affected by the derived term $\frac{X}{1+X}$. This term is a result of the nanoparticle residence time in the capillary being small compared to its residence time in tissue compartments. Therefore, the capillary is considered as a quasi-compartment and not taken into account during the derivation process.[48] The resulting term summarizes permeability between arterial/venous and tissue compartments.

Perfusion (flow)-limited versus Diffusion (membrane)-limited models

Generally, the PBPK model is either a diffusion-limited (permeability-limited) or a perfusion-limited (flow-limited) model.[49–51] However, in certain cases, it can be both. Perfusion-limited models are utilized where small lipophilic molecules can partition into tissues rapidly and the rate of blood flow is the limiting rate. Compounds that are large and hydrophilic have a harder time crossing the cell membrane and therefore diffusion-limited (membrane-limited) models would be utilized to model the disposition of those compounds.[18] On the other hand, hydrophobic or small compounds have an easier time crossing the cell membrane and thus perfusion-limited (or flow-limited) models would be utilized. In the case of gold nanoparticles, the proposed PBPK framework will be a membrane-limited model in order to take into account the rate limiting effects of nanoparticles crossing the cell membranes. Therefore, the model will describe the capillary blood and the tissue compartments separately.[48]

In diffusion-limited (membrane-limited) models, the rate of biodistribution depends on the permeability of the membrane with respect to the drug. However, in perfusion-limited (flow-limited) models, the rate-limiting step resides in the tissue partitioning of the drug. Identifying where the rate-limiting step will help to determine the paradigm of biodistribution of drugs. Further, the flow and connectivity

of the organs will provide an overall picture of the PBPK model where differential equations may be applied to reflect the connections between organ compartments.

SUBCOMPARTMENTALIZATION

Anatomic subcompartmentalization

It is beneficial to consider anatomic subcompartmentalization in some instances. For example, an intestinal model can anatomically break down the gut into subcompartments because enterocytes—which are intestinal absorptive cells—can line the walls of the stomach all the way to the colon.[52–55] This subcompartmentalization is important because the ultimate possible routes where the drug ends up after an oral administration may not only be excretion through the colon, but also absorption throughout the different anatomic subcompartments within the gut where the drug can travel into the hepatic portal vein. Subcompartmentalization details several different other compartments that exist within a main compartment of the PBPK model and thus helps to improve results leading to better model validation. Subcompartmentalization in PBPK modeling has also been performed in the lungs, dermal, and nasal tissue.[50,56,57] In one instance, modeling of pulmonary drug biodistribution where detailed subcompartments of different regions of the lungs, including the right and left lungs, and lower and upper airways have been considered.[50]

Physiological subcompartmentalization

Colloidal nanoparticles do not dissolve in the aqueous milieu and therefore will encounter the body's immune response via macrophage uptake. Macrophage uptake may also be taken into account in the PBPK model with a phagocytizing cell (PC) compartment, which will account for clearance of nanoparticle drugs. Currently, macrophage uptake is composed of two basic different steps, which include absorption governed by the rate constant k_{ab} and desorption governed by the rate constant k_{de} via the law of mass action[34] (shown in Figure 4). Absorbed nanoparticles are ultimately released by the macrophage. The resident amount of time that any foreign substance possesses in a particular organ tissue is reflected in the equilibrium between the absorption and desorption rates.

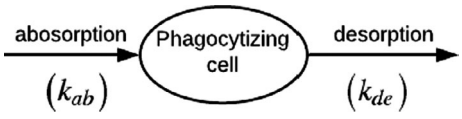

FIGURE 4 Phagocytizing cells as a physiological subcompartment within compartments with high concentrations of macrophage

Figure 4 shows the PCs being used as a physiological subcompartment. In these instances, the distribution equation for a compartment with high concentrations of macrophages, such as in the liver where there is high occurrence of Kuppfer cells, will need to account for the absorption and desorption processes:

$$\frac{dM_2}{dt} = Q \times \left(C_1 - \frac{C_2}{k_p}\right) \times \frac{X}{1+X} + \left[\left(k_{de} \times M_{2,m}\right) - \left(k_{ab} \times V_2 \times C_2\right)\right] \quad (6)$$

where $\boldsymbol{V}_2$ is the volume of organ in compartment 2; $\boldsymbol{C}_2$ is the concentration of nanoparticles in organ compartment 2; k_{ab} is the uptake rate of nanoparticles by phagocytizing cells in organ compartment 2; k_{de} is the desorption rate of nanoparticles by phagocytizing cells in organ compartment 2; and $M_{2,m}$ is the amount of nanoparticles captured by phagocytizing cells in organ compartment 2. Organ compartment 2 was used in this example for absorption and desorption because it represents the compartment containing the nanoparticle drugs being calculated.

Whereas some compartmental models currently used in the literature for PBPK modeling do account for macrophage uptake, these models may not account for the existence of confounding variables in the phagocytizing events. For instance, they may not consider the effects of adsorption and internalization, which can affect the maximum uptake constant. The importance of considering adsorption and internalization of nanoparticles when it comes to cellular uptake was demonstrated by Yeo and colleagues where differential labeling using electron microscopy revealed three different processes, including "attachment," "in between," and "internalized."[58] Wilhelm and colleagues have further approached the topic using superparamagnetic iron oxide nanoparticle's (SPIONS's) interactions with macrophages and built a mathematical framework around their adsorption and internalization kinetics.[59] The progression of the macrophage uptake process, including both adsorption and internalization, was validated further by epifluorescence microscopy.[58] Development of the subcompartmentalization of macrophage uptake can further be validated with semiqualitative data from the literature.[58] Much of the literature shows macrophage uptake data that includes consideration for absorption and desorption. For example, Liu et al. discusses a quantitative approach to obtaining absorption (k_{in}) and desorption (k_{out}) hepatic constants.[60] The current inclusion of macrophages as a "compartment" within PBPK modeling makes several assumptions, including homogeneity of macrophages' uptake rate. Additional consideration regarding what affects adsorption and

internalization may be helpful to understanding the overall phagocytizing process. Qie et al. have shown that surface modification of nanoparticles can influence phagocytic clearance.[61]

PARAMETERS

Non-nanoparticle specific parameters

Input parameters are key for PBPK model simulations. Input parameters describe three types of properties: physicochemical properties; drug-biological properties; and anatomic and physiological properties.[62] Parameters that come from physicochemical properties are drug-dependent and include the partition coefficient, pH-dependent partition coefficient, membrane affinity, molecular weight, equilibrium constants, and solubility.[49,62] Parameters that come from drug-biological properties depend on both drug and organism properties. These parameters include fraction of unbound drugs, Michaelis-Menten constant, dissociation constant, and maximum velocity. Because drug-biological properties depend not only on the organism but also the drugs, partition coefficients and permeability of drugs are also considered as drug-biological properties for they depend on both the organism and the physicochemical properties of the drug. Parameters deriving from anatomic or physiological properties (organ-specific) include organ volume, surface areas, tissue composition, blood flow rates, and expression levels.[63] Some of these parameters are used in PBPK modeling to predict the pharmacokinetic disposition for different populations. For example, expression levels can help determine the gene expression for a group of metabolizing enzymes in different organs for different populations.[62,64–69] Gene expression data may be represented as a normalized relative value with respect to the tissue or organ with the highest expression.[62] Thus, with different metabolizing enzyme expressions, results for clearance will be reflected in different populations having different levels of expression. Using gene expression data can aid the PBPK model in achieving resolution in the amount of metabolizing enzymes as well as other physiological parameters that aid in determining the dosing regimen.[64,65]

Nanoparticle-specific parameters

PBPK models built for nanoparticles will also include nanoparticle-specific parameters, which may include nanoparticle release constant, maximum uptake rate in phagocytic cells, Hill coefficient, and phagocytic cells release constant (desorption). Tables 1 and 2 show examples of important organ-specific and nanoparticle-specific parameters used in nanoparticle PBPK modeling.

TABLE 1 Typical organ-specific parameters used in both nanoparticle and non-nanoparticle PBPK modeling

Organ specific parameters	Unit	Value
Organ volumes based on % of body weight[a]		
Lungs	Liter	0.0001
Heart	Liter	9.5E−5
Brain	Liter	0.00017
Spleen	Liter	0.0001
Kidneys	Liter	0.00034
Liver	Liter	0.0013
Pancreas	Liter	0.00013
Stomach	Liter	0.00011
Arterial blood	Liter	0.000228182
Venous blood	Liter	0.000524818
Blood flow[b]		
Lungs	l/min	5.47E−3
Heart	l/min	2.80E−4
Brain	l/min	1.30E−4
Spleen	l/min	9.00E−5
Kidneys	l/min	1.30E−3
Liver	l/min	3.50E−4
Pancreas	l/min	5.20E−5
Stomach	l/min	1.10E−4
Portal vein	l/min	1.75E−3

Abbreviation: PBPK, physiologically-based pharmacokinetic.

[a]Can also be calculated by taking the percentage of the weight of a mouse in (g) to give the organ volume in (ml). Other sources in the literature include.[28,48,91–93] However, these values are based on 20 g mouse calculated by PK-Sim 8 database.

[b]Based on values obtained by PK-Sim 8 database for the mouse.

Some of the parameters, such as liver transporter kinetic data, metabolic enzymes (CYPs), permeability data, and transporter-mediated uptake, can be determined via in vitro experiments and then applied to different stages of absorption, distribution, metabolism, and excretion of the PBPK model to obtain simulated in vivo data.[50,51,70,71] More specifically, nanoparticle-related parameters, such as macrophage uptake rate and desorption rate constants, may be determined in vitro and then applied to a nanoparticle PBPK model.

Parameter estimation

Predicting biodistribution requires accurate input parameters. Although many parameters may be obtained through established literature sources, some cannot be relied upon

for predicting biodistribution. When nanoparticle pharmacokinetic disposition is needed for a new formulation, prior parameter estimates and some assumptions may be used. For example, blood flow may be obtained from the literature. Uptake capacity values may be recycled from PK parameters of nanoparticles with similar physical properties. However, one must use some caution in relying on predetermined nano-specific parameters when dealing with nanoparticles even with a slight change in the surface chemistry which can affect their interactions, for example, with macrophages or membranes, and thus can ultimately affect the macrophage uptake rate or permeability coefficients. Therefore, to obtain a good model fit to biodistribution data, a parameter optimization process is needed. For parameter optimization, only a select group of parameters would be required to be optimized. Because organ-specific parameters (Table 1) can readily be obtained from databases as well as being values of minimal variation, these parameters can be exempt from optimization. If we know the range of plausible values for a parameter being optimized, constraints may be added to the parameters being optimized. A variety of local and global optimization techniques can be found in the literature and implemented on MATLAB, for example.[72,73] Optimizing parameters will not only provide the best-fit model, it also allows the researcher to compare parameters under different nanoparticle formulations. Thus, providing a way to study the effects of different engineered nanoparticles on their corresponding estimated parameters.

Sensitivity analysis

Sensitivity analysis (SA) generates sensitivity indices for each of the parameters to gauge the effects on model output when input parameters are varied. The difference between global and local SAs is that local SA assesses variation in model output based on the changes of one parameter at a time (while all other parameters are held constant), whereas global SA examines not only the overall model response based on variation in all input parameters but also the variance in model output due to interactions between parameters. SA tests can help to reduce model complexity and elucidate highly sensitive parameters. Conceptually, SA tests for nanoparticle PBPK models should be the same as for non-nanoparticle ones. Nanoparticle-specific parameters, such as macrophage uptake absorption and desorption constants, may be of interest.

Local SA

Every PBPK model developed that reflects the specific virtual population as well as the nanoparticulate/

TABLE 2 An example of colloidal nanoparticle specific parameters taking into account the reticulo-endothelial system (macrophage uptake) of nanoparticles

	Description	Lungs	Heart	Liver	Kidneys	Spleen	Pancreas	Brain	Stomach
Nanoparticle specific parameters									
Unitless	Partition (distribution coefficient)[a]	0.15	0.15	0.08	0.15	0.15	0.15	0.15	0.15
Unitless	Permeability coefficient between blood and tissue[b]	0.001	0.000001	0.001	0.001	0.03	0.000001	0.000001	0.000001
h^{-1}	Max uptake rate constant for PC[b]	Generic	Generic	Generic	Generic	0.112 ± 0.000990	Generic	Generic	Generic
h^{-1}	PC release (desorption) rate constant[b]	Generic	Generic	Generic	Generic	Generic	Generic	Generic	Generic
L/h	Excretion rate constant[c]	N/A	N/A	1.18 × 10–2 ± 2.92 × 10–4	6.56 × 10–3 ± 5.35 × 10–5	N/A	N/A	N/A	N/A

Note: According to Li and other sources in the literature, arterial and venous blood take up 20% and 80% of the total body blood, respectively.[31,48]

[a]Taken from the table in ref. 31 which also come from other sources. Source provides data for the liver, spleen, kidneys, lungs, brain, and the rest of the body. Therefore, any organ compartment not directly provided by source, rest of the body values are used.

[b]Values obtained from ref. 83. Some assumptions were made since these values were used for rats under different colloidal nanoparticles. Generic values are equal to 16.1 ± 0.306 for absorption and $4.90 \times 10^{-19} \pm 7.26 \times 10^{-17}$ for desorption.

[c]Values obtained from ref. 83

nonparticulate drug system used will have a unique concentration-time curve for any particular compartment based on the input parameters. The degree of influence of a parameter on the concentration-time curve may not be obvious without an SA. Typically, two approaches have been used for local PBPK SA tests. One approach is to multiply or divide each parameter by a predetermined value and observe the concentration output or amount of nanoparticles in each of the compartment with respect to time. Another approach is to measure the change in the area under the curve (AUC) after a 1% change in the parameter value.[34,74] More specifically:

$$\text{Sensitivity Coefficient} = \frac{\text{dAUC}/\text{AUC}}{\text{d}p/p} \tag{7}$$

where AUC is the area under the concentration-time curve in a compartment and dAUC is the change in AUC of that compartment reflecting a 1% change in the parameter $\text{d}p/p = 0.01$.[34,74,75] When conducting a sensitivity analysis, the higher the sensitivity coefficient for a parameter, the larger the influence of that parameter on the model output for a particular compartment. However, the equation above only gives the local sensitivity coefficient. A more global and systematic approach to sensitivity analysis is needed to show the influence of a parameter over a set of all possible input parameters.[76] Further, local sensitivity analysis is only appropriate when interactions between parameters are negligible.[76]

Global SA

Global sensitivity analysis (GSA) falls into one of two categories, which are elementary effect and variance-based GSA methods.[77] Two GSA methods have been used in PBPK modeling are the Morris screening (an elementary effect method) and the extended Fourier Amplitude Sensitivity Test (eFAST; a variance-based method), which can be used to study the effects of input parameters on pharmacokinetic outputs.[77–79] The Morris test is a qualitative test to identify noninfluential input parameters in PBPK modeling, which can be fixed without consequences on output uncertainty. It is a preliminary test typically used as a first step in some PBPK global sensitivity analyses within a GSA workflow giving rough estimations with a limited number of calculations.[76–78] The Morris method gives two measures of sensitivity consisting of (μ) which measures a variable's overall influence and (σ) which approximates the nonlinear effects of the variables in the model which are then plotted on a σ versus μ plot.[80] Using the Morris method (Figure 5), simulations that yield low measures of μ and low measures of σ indicate that the input parameter has a negligible effect; simulations that yield high μ but low σ indicate that whereas the parameter is sensitive, it still has very little interaction with other parameters, or that it has linear effects; and simulations that yield both high μ and high σ indicate parameters that are both sensitive and either interact with other parameters or are nonlinear.[81]

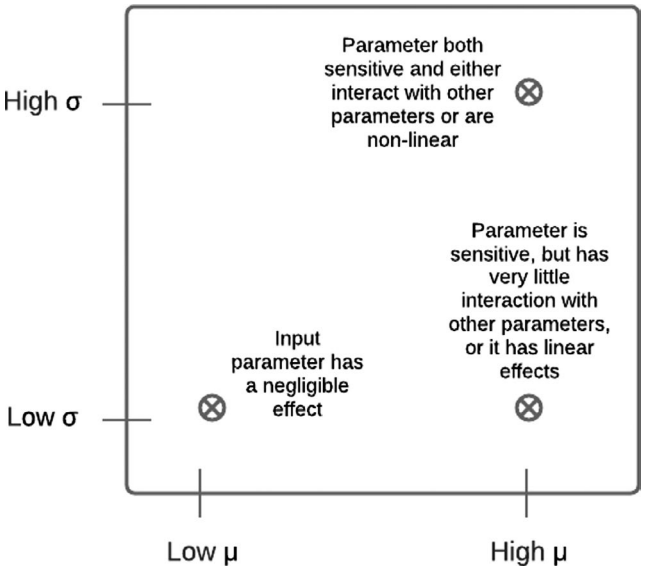

FIGURE 5 Results of the Morris method, a qualitative test, can be visualized on a σ versus μ plot. Only simulations that yield both high σ and μ indicate parameters are both sensitive and either interact with other parameters or are nonlinear

On the other hand, the eFAST method is a quantitative method for a subset of explanatory selected parameters. These selected parameters may be chosen from the previously discussed Morris method. McNally and colleagues demonstrated the use of Lowry plots to display how much variances may be accounted for in model outputs if all parameters are included up a certain point within the plot as well as discusses the calculation of the upper and lower bounds of the variances.[76] More common GSA methods may also be applied to nanoparticle PBPK model development to assess outlier or counterintuitive effects of certain parameters on the model. Good practice in GSA application includes applying multiple methods, reiterating choices made, and graphically visualizing results for effective communication of parameter influences.[82]

MODEL VALIDATION

Model validation takes place after key parameters have been determined by either performing parameter estimation or obtained through previous literature findings. This

essentially means that validation requires a different set of empirical data in order to validate the model built on previous findings or assumptions.

The R^2 analysis is typically used to evaluate a model which is based on the deviation from the line of unity between $\log_{10}$ of measured and predicted values. Geometric standard deviations (GSD^2) may also be used to further validate a model. A GSD^2 less than 10 will indicate that the accuracies of prediction of individual data points are of maximum one order of magnitude, for instance.[83] Additionally, results of PBPK models may also be validated based on either looking at the percent (%) errors or fold errors. The AUC and maximum concentrations (C_{max}) and clearance (CL) are all model outputs that can be used in the validation discussion. Percent error is the measure of the difference in predicted and actual values over the predicted values. These values may be lowered after optimization of a model. For example, Mavroudis and colleagues showed that in three different formulations of paracetamol, by lowering the gastric emptying time (GET) and dissolution time (DT), and by altering the dissolution shape (DS) parameter, they were able to decrease the percent error of results which were previously obtained by a different group.[84] Optimization of models is a way to further elucidate our understanding of the impact of our parameters.

Another method of analyzing the validity of models is through the use of average fold-errors, which are ratios of predicted over observed values.[85] This method is typically used in analyzing the validity of predicted CL and other model outputs where a 2.0 or less fold-error is preferred.[85,86] The absolute average fold error (AAFE) is the average of all fold errors for a particular model output[87]:

$$\text{Absolute Average Fold Error (AAFE)} = 10^{\frac{1}{n}\sum\left|\log\frac{\text{predicted}}{\text{observed}}\right|}$$

where n is the size of the data. The AAFE value may be plotted with its SD. In one example, Zhou and colleagues have analyzed the performance of model in six different age groups under four different drugs which yielded a 0.5–2.0 fold-error[85]: The closer to the predicted/observed ratio of 1.0 along with variations not extending beyond a predetermined range, in this case, 0.5–2.0, the more confidence we have in the model. Other ways to analyze the model based on fold-errors is to plot the percentage of data points falling within a 2.0 fold-error or plotting absolute average fold-errors of model outputs by various model approaches.[87] It is important to note the optimization of a model depends on the reiteration of that model based on improved understanding of parameter influences as well as error analysis results. Therefore, effective PBPK model development is a workflow that relies on our understanding of: how to build the model structure mechanistically, the mathematical framework underlying the biodistribution of the nanoparticles, the importance of the contributions of each of the parameters, and how to evaluate the effectiveness of the model through model validation methods.

INTERSPECIES EXTRAPOLATION

Although there are a plethora of available in vivo pharmacokinetic data deriving from rodent studies that can be used as an empirical aspect to PBPK model development, there remains translational questions regarding how to further our elucidation of biodistribution investigations and apply that in the clinical setting. Part of the reason for PBPK modeling is to circumvent the need for excessive animal studies, and thereby reduce the resources needed to obtain information on dosing, for example. Mechanistic PBPK modeling has presented more of a first-principles approach to modeling and simulating nanoparticle drug biodistribution. Therefore, its interspecies extrapolation to humans also requires a more mechanistic approach, compared to that of traditional allometric scaling. Allometric scaling only takes into account weight and size factors but not fundamental biochemical mechanisms, and therefore does not offer much more than "black box" inter- and intra-species extrapolation.[88] Hall et al. proposed a multiscale biological system model describing not only the fate of drugs in cells, tissues, organs, and the whole body, but also intra- and interspecies by scaling: hepatocytes to account for metabolic activity; mass transport area to account for mass transfer of active transport; and remaining physiological and anatomic parameters to account for biodistribution across species.[88] Lin et al. also presented interspecies extrapolation by scaling physiological and endocytic parameters while keeping nanoparticle-specific parameters the same.[89] Whereas it is possible to scale endocytic parameters based on the macrophage's occurrence within an organ tissue, their specific kinetic parameters may be experimentally determined, albeit, with a few suggestions. For example, primary cell types are preferred over immortalized cell lines, and a time-dependent study to determine when the cells are at maximum uptake rate as well as a concentration-dependent study to determine macrophage uptake kinetics.[89]

CONCLUSION

This tutorial paper gives an overview of how to build a PBPK model for nanoparticle drugs using a flow diagram decision-making process which requires an understanding of the nanoparticle physicochemical nature. The main components of a PBPK model comprises the model structure and the pharmacokinetic mathematical framework. Both the model structure and the mathematical framework are built based on several initial questions which

are: whether the nanoparticle drugs are dissolvable or colloidal; and, if so, whether the dissolved nanoparticle drug is a large or molecular hydrophilic drug. Specifically, dissolvable nanoparticles will need a release term to account for the increase in the amount of drug molecules from nanoparticle dissolution. Further, the model for dissolvable nanoparticles will either take on perfusion-limited or membrane-limited structures. Consequently, membrane-limited models do not have a permeability term because blood flow to the organs are the limiting step in the model. Because colloidal nanoparticles do not undergo dissolution, a membrane-limited model is assumed. Within the model structure, anatomic and physiological subcompartmentalization may be applied, and, thus, add further complexity to the model. The rest of the model-building process comprises of looking at appropriate general and nanoparticle-specific parameters, an overview of sensitivity analysis as well as model validation. With a more streamlined approach to building a PBPK model, as synthesized in this paper, understanding and working with pharmacokinetic modeling can be enhanced.

CONFLICT OF INTEREST

The authors declared no competing interests for this work.

ORCID

Anh-Dung Le https://orcid.org/0000-0003-0771-2759

REFERENCES

1. Perrault SD, Chan WCW. In vivo assembly of nanoparticle components to improve targeted cancer imaging. *Proc Natl Acad Sci USA*. 2010;107:11194-11199.
2. Jing H, Sinha S, Sachar HS, Das S. Interactions of gold and silica nanoparticles with plasma membranes get distinguished by the van der Waals forces: Implications for drug delivery, imaging, and theranostics. *Colloids Surf B Biointerfaces*. 2019;177:433-439.
3. Stephen ZR, Kievit FM, Zhang M. Magnetite nanoparticles for medical MR imaging. *Mater Today Kidlington Engl*. 2011;14:330-338.
4. Hossen S, Hossain MK, Basher MK, Mia MNH, Rahman MT, Uddin MJ. Smart nanocarrier-based drug delivery systems for cancer therapy and toxicity studies: a review. *J Adv Res*. 2019;15:1-18.
5. Sonavane G, Tomoda K, Makino K. Biodistribution of colloidal gold nanoparticles after intravenous administration: Effect of particle size. *Colloids Surf B Biointerfaces*. 2008;66:274-280.
6. Takeuchi I, Onaka H, Makino K. Biodistribution of colloidal gold nanoparticles after intravenous injection: Effects of PEGylation at the same particle size. *Biomed Mater Eng*. 2018;29:205-215.
7. Dong D, Wang X, Wang H, Zhang X, Wang Y, Wu B. Elucidating the in vivo fate of nanocrystals using a physiologically based pharmacokinetic model: a case study with the anticancer agent SNX-2112. *Int J Nanomedicine*. 2015;10:2521-2535.
8. US Food and Drug Administration. Physiologically Based Pharmacokinetic Analyses — Format and Content Guidance for Industry. September 2018. https://doi.fda.gov/regulatory-information/search-fda-guidance-documents/physiologically-based-pharmacokinetic-analyses-format-and-content-guidance-industry
9. Davda JP, Jain M, Batra SK, Gwilt PR, Robinson DH. A physiologically based pharmacokinetic (PBPK) model to characterize and predict the disposition of monoclonal antibody CC49 and its single chain Fv constructs. *Int Immunopharmacol*. 2008;8:401-413.
10. Heiskanen T, Heiskanen T, Kairemo K. Development of a PBPK model for monoclonal antibodies and simulation of human and mice PBPK of a radiolabelled monoclonal antibody. *Curr Pharm Des*. 2009;15:988-1007.
11. Dogra P, Butner JD, Nizzero S, et al. Image-guided mathematical modeling for pharmacological evaluation of nanomaterials and monoclonal antibodies. *Wiley Interdiscip Rev Nanomed Nanobiotechnol* 2020;12:e1628.
12. Korzekwa K, Nagar S. On the nature of physiologically-based pharmacokinetic models –A Priori or A posteriori? Mechanistic or Empirical? *Pharm Res*. 2017;34:529-534.
13. Ono C, Hsyu P-H, Abbas R, Loi C-M, Yamazaki S. Application of physiologically based pharmacokinetic modeling to the understanding of bosutinib pharmacokinetics: prediction of drug-drug and drug-disease interactions. *Drug Metab Dispos*. 2017;45:390-398.
14. Chen Y, Mao J, Hop CECA. Physiologically based pharmacokinetic modeling to predict drug-drug interactions involving inhibitory metabolite: a case study of amiodarone. *Drug Metab Dispos*. 2014;43:182-189.
15. Galetin A, Zhao P, Huang S-M. Physiologically based pharmacokinetic modeling of drug transporters to facilitate individualized dose prediction. *J Pharm Sci*. 2017;106:2204-2208.
16. Kostewicz ES, Aarons L, Bergstrand M, et al. PBPK models for the prediction of in vivo performance of oral dosage forms. *Eur J Pharm Sci*. 2014;57:300-321.
17. Yang F, Wang B, Liu Z, et al. Prediction of a therapeutic dose for buagafuran, a Potent anxiolytic agent by physiologically based pharmacokinetic/pharmacodynamic modeling starting from pharmacokinetics in rats and human. *Front Pharmacol*. 2017;8:683.
18. Peters SA. Evaluation of a generic physiologically based pharmacokinetic model for lineshape analysis. *Clin Pharmacokinet*. 2008;47:261-275.
19. Zhuang X, Lu C. PBPK modeling and simulation in drug research and development. *Acta Pharm Sin B*. 2016;6:430-440.
20. Liang X, Wang H, Grice JE, et al. Physiologically based pharmacokinetic model for long-circulating inorganic nanoparticles. *Nano Lett*. 2016;16:939-945.
21. Henrique SA, Lima EJ, Mansilla MV, et al. A physiologically based pharmacokinetic model to predict the superparamagnetic iron oxide nanoparticles (SPIONs) accumulation in vivo. *Eur J Nanomedicine*. 2017;9:79-90.
22. Glassman PM, Balthasar JP. Physiologically-based pharmacokinetic modeling to predict the clinical pharmacokinetics of monoclonal antibodies. *J Pharmacokinet Pharmacodyn*. 2016;43:427-446.
23. Stader F, Penny MA, Siccardi M, Marzolini C. A comprehensive framework for physiologically-based pharmacokinetic modeling in Matlab. *CPT Pharmacomet Syst Pharmacol*. 2019;8:444-459.

24. Zang X, Kagan L. Physiologically-based modeling and interspecies prediction of paclitaxel pharmacokinetics. *J Pharmacokinet Pharmacodyn*. 2018;45:577-592.
25. Bi Y, Deng J, Murry DJ, An G. A whole-body physiologically based pharmacokinetic model of gefitinib in mice and scale-up to humans. *AAPS J*. 2016;18:228-238.
26. Tylutki Z, Polak S. A four-compartment PBPK heart model accounting for cardiac metabolism - model development and application. *Sci Rep*. 2017;7:39494.
27. Kagan L, Gershkovich P, Wasan KM, Mager DE. Physiologically based pharmacokinetic model of amphotericin B disposition in rats following administration of deoxycholate formulation (Fungizone®): pooled analysis of published data. *AAPS J*. 2011;13:255.
28. Sweeney LM, Thrall KD, Poet TS, et al. Physiologically based pharmacokinetic modeling of 1,4-dioxane in rats, mice, and humans. *Toxicol Sci*. 2008;101:32-50.
29. Pawar VK, Singh Y, Meher JG, Gupta S, Chourasia MK. Engineered nanocrystal technology: In-vivo fate, targeting and applications in drug delivery. *J Controlled Release*. 2014;183:51-66.
30. Muller RH, Keck CM. Challenges and solutions for the delivery of biotech drugs – a review of drug nanocrystal technology and lipid nanoparticles. *J Biotechnol*. 2004;113:151-170.
31. Lin Z, Monteiro-Riviere NA, Riviere JE. A physiologically based pharmacokinetic model for polyethylene glycol-coated gold nanoparticles of different sizes in adult mice. *Nanotoxicology*. 2016;10:162-172.
32. Di Muria M, Lamberti G, Titomanlio G. Physiologically based pharmacokinetics: a simple, all purpose model. *Ind Eng Chem Res*. 2010;49:2969-2978.
33. Gilkey M, Krishnan V, Scheetz L, Jia X, Rajasekaran AK, Dhurjati PS. Physiologically based pharmacokinetic modeling of fluorescently labeled block copolymer nanoparticles for controlled drug delivery in leukemia therapy: physiologically based pharmacokinetic modeling. *CPT Pharmacomet Syst Pharmacol*. 2015;4:e00013.
34. Li D, Morishita M, Wagner JG, et al. In vivo biodistribution and physiologically based pharmacokinetic modeling of inhaled fresh and aged cerium oxide nanoparticles in rats. *Part Fibre Toxicol*. 2016;13:45.
35. Bardal SK, Waechter JE, Martin DS. Chapter 2 - pharmacokinetics. In Bardal SK, Waechter JE, Martin DS, eds. *Applied Pharmacology*. Content Repository Only! Elsevier; 2011:17-34.
36. Cedervall T, Lynch I, Lindman S, et al. Understanding the nanoparticle-protein corona using methods to quantify exchange rates and affinities of proteins for nanoparticles. *Proc Natl Acad Sci USA*. 2007;104:2050-2055.
37. del Pino P, Pelaz B, Zhang Q, Maffre P, Nienhaus GU, Parak WJ. Protein corona formation around nanoparticles – from the past to the future. *Mater Horiz*. 2014;1:301-313.
38. Ke PC, Lin S, Parak WJ, Davis TP, Caruso F. A decade of the protein corona. *ACS Nano*. 2017;11:11773-11776.
39. Barbero F, Russo L, Vitali M, et al. Formation of the protein corona: the interface between nanoparticles and the immune system. *Semin Immunol*. 2017;34:52-60.
40. Zhdanov VP, Cho N-J. Kinetics of the formation of a protein corona around nanoparticles. *Math Biosci*. 2016;282:82-90.
41. Bertrand N, Grenier P, Mahmousi M, et al. Mechanistic understanding of in vivo protein corona formation on polymeric nanoparticles and impact on pharmacokinetics. *Nat Commun*. 2017;8:777.
42. Bros M, Nuhn L, Simon J, et al. The protein corona as a confounding variable of nanoparticle-mediated targeted vaccine delivery. *Front Immunol*. 2018;9:1760.
43. Sahneh FD, Scoglio CM, Monteiro-Riviere NA, Riviere JE. Predicting the impact of biocorona formation kinetics on interspecies extrapolations of nanoparticle biodistribution modeling. *Nanomed*. 2015;10:25-33.
44. Dogra P, Adolphi NL, Wang Z, et al. Establishing the effects of mesoporous silica nanoparticle properties on in vivo disposition using imaging-based pharmacokinetics. *Nat Commun*. 2018;9:4551.
45. Carter P, Narasimhan B, Wang Q. Biocompatible nanoparticles and vesicular systems in transdermal drug delivery for various skin diseases. *Int J Pharm*. 2019;555:49-62.
46. Han G, Ghosh P, Rotello VM. Functionalized gold nanoparticles for drug delivery. *Nanomed*. 2007;2:113-123.
47. Yu X, Trase I, Ren M, Duval K, Guo X, Chen Z. Design of nanoparticle-based carriers for targeted drug delivery. *J Nanomater*. 2016;2016:1087250.
48. Li D, Johanson G, Emond C, Carlander U, Philbert M, Jolliet O. Physiologically based pharmacokinetic modeling of polyethylene glycol-coated polyacrylamide nanoparticles in rats. *Nanotoxicology*. 2014;8 Suppl 1:128-137.
49. Li M, Al-Jamal KT, Kostarelos K, Reineke J. Physiologically based pharmacokinetic modeling of nanoparticles. *ACS Nano*. 2010;4:6303-6317.
50. Gaohua L, Wedagedera J, Small BG, et al. Development of a multicompartment permeability-limited lung PBPK model and its application in predicting pulmonary pharmacokinetics of antituberculosis drugs: lung PBPK model. *CPT Pharmacomet Syst Pharmacol*. 2015;4:605-613.
51. Cheng W, Ng CA. A permeability-limited physiologically based pharmacokinetic (PBPK) model for perfluorooctanoic acid (PFOA) in male rats. *Environ Sci Technol*. 2017;51:9930-9939.
52. Lin L, Wong H. Predicting oral drug absorption: mini review on physiologically-based pharmacokinetic models. *Pharmaceutics*. 2017;9:41.
53. Jones H, Rowland-Yeo K. Basic concepts in physiologically based pharmacokinetic modeling in drug discovery and development. *CPT Pharmacomet Syst Pharmacol*. 2013;2:e63.
54. Krauss M, Tappe K, Schuppert A, Kuepfer L, Goerlitz L. Bayesian population physiologically-based pharmacokinetic (PBPK) approach for a physiologically realistic characterization of interindividual variability in clinically relevant populations. *PLoS One*. 2015;10:e0139423.
55. Cherkaoui-Rbati MH, Paine SW, Littlewood P, Rauch C. A quantitative systems pharmacology approach, incorporating a novel liver model, for predicting pharmacokinetic drug-drug interactions. *PLoS One*. 2017;12:e0183794.
56. Bookout RL Jr, McDaniel CR, Quinn DW, McDougal JN. Multilayered dermal subcompartments for modeling chemical absorption. *SAR QSAR Environ Res*. 1996;5:133-150.
57. Andersen ME, Green T, Frederick CB, Bogdanffy MS. Physiologically based pharmacokinetic (PBPK) models for nasal tissue dosimetry of organic esters: assessing the state-of-knowledge and risk assessment applications with Methyl Methacrylate and Vinyl Acetate. *Regul Toxicol Pharmacol*. 2002;36:234-245.

58. Yeo JC, Wall AA, Stow JL, Hamilton NA. High-throughput quantification of early stages of phagocytosis. *Biotechniques*. 2013;55(3):115-124.
59. Wilhelm C, Gazeau F, Roger J, Pons JN, Bacri J-C. Interaction of anionic superparamagnetic nanoparticles with cells: kinetic analyses of membrane adsorption and subsequent internalization. *Langmuir*. 2002;18:8148-8155.
60. Liu T, Choi H, Zhou R, Chen I-W. Quantitative evaluation of the reticuloendothelial system function with dynamic MRI. *PLoS One*. 2014;9:e103576.
61. Qie Y, Yuan H, von Roemeling CA, et al. Surface modification of nanoparticles enables selective evasion of phagocytic clearance by distinct macrophage phenotypes. *Sci Rep*. 2016;6:26269.
62. Kuepfer L, Niederalt C, Wendl T, et al. Applied concepts in PBPK modeling: how to build a PBPK/PD model: applied concepts in PBPK modeling. *CPT Pharmacomet Syst Pharmacol*. 2016;5:516-531.
63. Tsamandouras N, Rostami-Hodjegan A, Aarons L. Combining the 'bottom up' and 'top down' approaches in pharmacokinetic modelling: fitting PBPK models to observed clinical data: Parameter estimation in PBPK models. *Br J Clin Pharmacol*. 2015;79:48-55.
64. Wang X. Extrapolation of a PBPK model for dioxins across dosage regimen, gender, strain, and species. *Toxicol Sci*. 2000;56:49-60.
65. Meyer M, Schneckener S, Ludewig B, Kuepfer L, Lippert J. Using expression data for quantification of active processes in physiologically based pharmacokinetic modeling. *Drug Metab Dispos*. 2012;40:892-901.
66. Thiel C, Schneckener S, Krauss M, et al. A systematic evaluation of the use of physiologically based pharmacokinetic modeling for cross-species extrapolation. *J Pharm Sci*. 2015;104:191-206.
67. Rioux N, Waters NJ. Physiologically based pharmacokinetic modeling in pediatric oncology drug development. *Drug Metab Dispos*. 2016;44:934-943.
68. Marsousi N, Desmeules JA, Rudaz S, Daali Y. Usefulness of PBPK modeling in incorporation of clinical conditions in personalized medicine. *J Pharm Sci*. 2017;106:2380-2391.
69. Andersen ME, Black MB, Campbell JL, et al. Combining transcriptomics and PBPK modeling indicates a primary role of hypoxia and altered circadian signaling in dichloromethane carcinogenicity in mouse lung and liver. *Toxicol Appl Pharmacol*. 2017;332:149-158.
70. Jamei M, Bajot F, Neuhoff S, et al. A mechanistic framework for in vitro–in vivo extrapolation of liver membrane transporters: prediction of drug-drug interaction between rosuvastatin and cyclosporine. *Clin Pharmacokinet*. 2014;53:73-87.
71. Yeo KR, Kenny JR, Rostami-Hodjegan A. Application of in vitro-in vivo extrapolation (IVIVE) and physiologically based pharmacokinetic (PBPK) modelling to investigate the impact of the CYP2C8 polymorphism on rosiglitazone exposure. *Eur J Clin Pharmacol*. 2013;69:1311-1320.
72. Supported Methods for Parameter Estimation in SimBiology - MATLAB & Simulink. Accessed November 1, 2020. https://www.mathworks.com/help/simbio/ug/supported-methods-for-parameter-estimation.html#responsive_offcanvas
73. MathWorks. Optimization Toolbox. 332. https://www.mathworks.com/products/optimization.html
74. Carlander U, Li D, Jolliet O, Emond C, Johanson G. Toward a general physiologically-based pharmacokinetic model for intravenously injected nanoparticles. *Int J Nanomedicine*. 2016;11:625-640.
75. Li M, Panagi Z, Avgoustakis K, Reineke J. Physiologically based pharmacokinetic modeling of PLGA nanoparticles with varied mPEG content. *Int J Nanomedicine*. 2012;7:1345-1356.
76. McNally K, Cotton R, Loizou GD. A workflow for global sensitivity analysis of PBPK models. *Front Pharmacol*. 2011;2:31.
77. Liu D, Li L, Jamei M. Application of Global Sensitivity Analysis Methods to Determine the most Influential Parameters of a Minimal PBPK Model of Quinidine. https://www.certara.com/app/uploads/2017/06/Liu_2017_PAGE_quinidine.pdf
78. Hsieh N-H, Reisfeld B, Bois FY, Chiu WA. Applying a global sensitivity analysis workflow to improve the computational efficiencies in physiologically-based pharmacokinetic modeling. *Front Pharmacol*. 2018;9:588.
79. Scherholz ML, Forder J, Androulakis IP. A framework for 2-stage global sensitivity analysis of GastroPlus™ compartmental models. *J Pharmacokinet Pharmacodyn*. 2018;45:309-327.
80. Lumen A, McNally K, George N, Fisher JW, Loizou GD. Quantitative global sensitivity analysis of a biologically based dose-response pregnancy model for the thyroid endocrine system. *Front Pharmacol*. 2015;6:107.
81. Iooss B, Lemaître P. A review on global sensitivity analysis methods. In: Dellino G, Meloni C, eds. *Uncertainty Management in Simulation-Optimization of Complex Systems*, vol. 59. Springer US; 2015:101-122.
82. Pianosi F, Sarrazin F, Wagener T. A Matlab toolbox for global sensitivity analysis. *Environ Model Softw*. 2015;70:80-85.
83. Li D. A Physiologically Based Pharmacokinetic Model Study of the Biological Fate, Transport and Behavior of Engineered Nanoparticles. https://deepblue.lib.umich.edu/handle/2027.42/111631
84. Mavroudis PD, Hermes HE, Teutonico D, Preuss TG, Schneckener S. Development and validation of a physiology-based model for the prediction of pharmacokinetics/toxicokinetics in rabbits. *PLoS One*. 2018;13:e0194294.
85. Zhou W, Johnson TN, Xu H, et al. Predictive performance of physiologically based pharmacokinetic and population pharmacokinetic modeling of renally cleared drugs in children: PBPK and PopPK pediatric modeling. *CPT Pharmacomet Syst Pharmacol*. 2016;5:475-483.
86. Daga PR, Bolger MB, Haworth IS, Clark RD, Martin EJ. Physiologically based pharmacokinetic modeling in lead optimization. 2. Rational bioavailability design by global sensitivity analysis to identify properties affecting bioavailability. *Mol Pharm*. 2018;15:831-839.
87. Zou P, Yu Y, Zheng N, et al. Applications of human pharmacokinetic prediction in first-in-human dose estimation. *AAPS J*. 2012;14:262-281.
88. Hall C, Lueshen E, Mošat A, Linninger AA. Interspecies scaling in pharmacokinetics: a novel whole-body physiologically based modeling framework to discover drug biodistribution mechanisms in vivo. *J Pharm Sci*. 2012;101:1221-1241.
89. Lin Z, Monteiro-Riviere NA, Kannan R, Riviere JE. A computational framework for interspecies pharmacokinetics, exposure and toxicity assessment of gold nanoparticles. *Nanomed*. 2016;11:107-119.
90. Lyons MA, Reisfeld B, Yang RSH, Lenaerts AJ. A physiologically based pharmacokinetic model of Rifampin in mice. *Antimicrob Agents Chemother*. 2013;57:1763-1771.

91. Brown RP, Delp MD, Lindstedt SL, Rhomberg LR, Beliles RP. Physiological parameter values for physiologically based pharmacokinetic models. *Toxicol Ind Health*. 1997;13:407-484.
92. Utturkar A, Paul B, Akkiraju H, Bonor J, Dhurjati P, Nohe A. Development of Physiologically Based Pharmacokinetic Model (PBPK) of BMP2 in Mice. *Biol Syst Open Access*. 2013;2:1000123.
93. Kirman CR, Hays SM, Aylward LL, et al. Physiologically based pharmacokinetic model for rats and mice orally exposed to chromium. *Chem Biol Interact*. 2012;200:45-64.

How to cite this article: Le A-D, Wearing HJ, Li D. Streamlining physiologically-based pharmacokinetic model design for intravenous delivery of nanoparticle drugs. *CPT Pharmacometrics Syst Pharmacol*. 2022;11:409-424. doi:10.1002/psp4.12762